

Delaminated Layered Double Hydroxide Delivers DNA Molecules as
Sandwich Nanostructure into Cells via a Non-endocytic Pathway

Ye Li^{1#*}, Wenlong Bao^{1#}, Hongyang Wu¹, Junya Wang², Yu Zhang³, Yinglang Wan¹,
Dapeng Cao⁴, Dermot O'Hare⁵, Qiang Wang^{3*}

¹College of Biological Sciences and Biotechnology, Beijing Forestry University, 35
Qinghua East Road, Haidian District, Beijing 100083, P. R. China.

²Faculty of Environmental Science and Engineering, Kunming University of Science and
Technology, Kunming, 650500, Yunnan, P. R. China.

³College of Environmental Science and Engineering, Beijing Forestry University, 35
Qinghua East Road, Haidian District, Beijing 100083, P. R. China.

⁴State Key Laboratory of Organic-Inorganic Composites, Beijing University of Chemical
Technology, Beijing 100029, P. R. China.

⁵Chemistry Research Laboratory, Department of Chemistry, University of Oxford,
Mansfield Road, Oxford OX1 3TA, United Kingdom.

[#]Authors contribute equally to this work.

*Corresponding authors:

Professor Ye Li:

E-mail: li.ye.0223@163.com; liye0223@bjfu.edu.cn

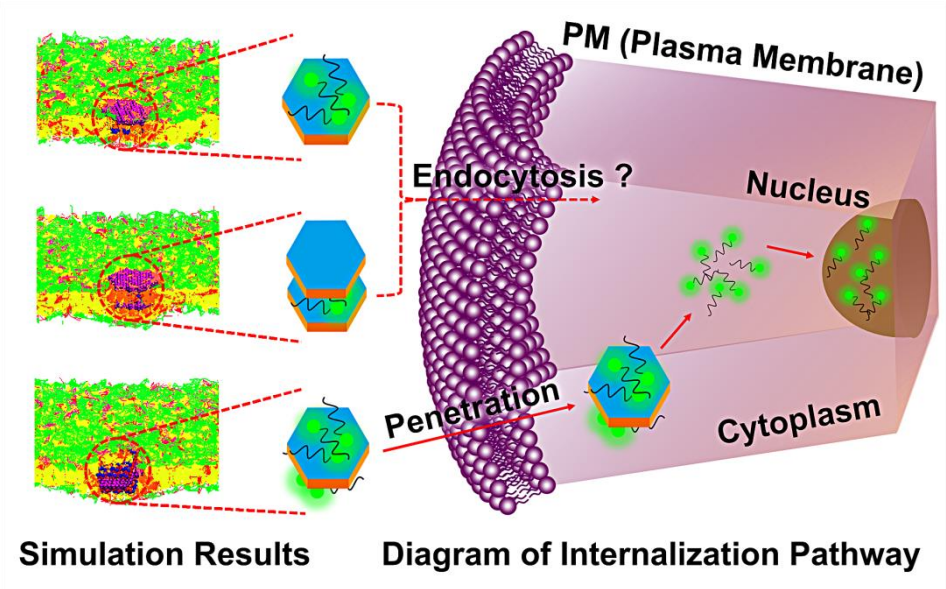
Tel: +86 15201216656

Professor Qiang Wang

E-mail: qiang.wang.ox@gmail.com; qiangwang@bjfu.edu.cn

Tel: +86 13699130626

Graphic Abstract



Abstract

Layered double hydroxides (LDHs) are effective molecular carriers in cytological research, gene therapy, and transgenic applications. Herein, we investigated the internalization behavior of the LDH-DNA bioconjugates via a microscopic approach and analyzed the internalization pathway by dissipative particle dynamics (DPD) simulations. We experimentally found that LDH can efficiently carry DNA into the nucleus of cell in BY-2 suspension cells. Furthermore, atomic force microscopy and X-ray diffraction analysis demonstrated that the LDH-DNA bioconjugates mainly exist as a DNA-LDH-DNA sandwich complex, while the LDH-DNA-LDH sandwich complex and DNA-LDH complex cannot be excluded. The DPD simulations further indicated that only the DNA-LDH-DNA sandwich structure could penetrate the plasma membrane (PM), while PM is impermeable to the LDH-DNA-LDH sandwich complex and the DNA-LDH complex. This work provides novel perspective for understanding the membrane penetration mechanism of LDH nano-sheets and new insights into the design of novel molecular delivery systems.

Keywords: Layered double hydroxides, DNA, gene delivery, effective penetration structure, dissipative particle dynamics simulations

1. Introduction

Nanomaterials-based molecular delivery systems have been widely used in current biological and medical applications[1-3]. The key for designing an effective molecular delivery system is to find suitable nanomaterials that have a high capacity to the target molecules, exhibit high penetration efficiency, and induce low damage to the biological barriers, i.e., the plasma membrane (PM)[4, 5]. Therefore, a better understanding of the nanomaterials' internalization mechanism into cytosols and the interaction mechanism between nanomaterials and the lipid membrane is urgently required.

Nanomaterials such as drug/gene delivery carriers usually enter the cell via penetration, actin-based phagocytosis, clathrin-mediated or lipid raft-mediated endocytosis[6-9]. In the endocytotic and phagocytotic pathways, nanoparticles are engulfed within vesicular structures surrounded by lipid membranes. Subsequently, these vesicles may directly target those nanomaterials to intracellular compartments and organelles. These include lysosomes (or vacuoles in plant cells) that can rapidly destroy biomolecules[10]. To transport the membrane-impermeable biomolecules (MIBs) into the designated cell organelles and to help MIBs escape from the lysosomes of the target cells, researchers have developed cell-penetrating peptides and proteins[11, 12], endosome-disruptive polymers[13], and endosomal/lysosomal escaping lipids[14]. Control of structure, shape, and stability of nanotransporters is critically important because those parameters determine their bio-distribution and cytotoxicity *in vivo*[15].

Due to the good biocompatibility, low cytotoxicity, high anion exchange capacity, and pH-controlled release of guest molecules, the use of layered double hydroxides (LDHs) as efficient nanotransporters for DNA, RNA, and pharmaceuticals has attracted

great attention recently[16-20]. The positively charged surface of LDH nanosheets can absorb negatively charged material and form neutral bioconjugates[21]. The DNA molecules are thought to be inserted into the inter-layers of LDH nanosheets with a stabilized structure[19]. The size and surface properties of LDH nanosheets can affect the capacity of LDHs to target molecules and penetrate the PM[16, 22]. The delaminated LDH nanosheet not only efficiently carries the DNA molecules into the animal cells, but it can also deliver target molecules into the cell wall surrounding plant cells. This is another important application of LDHs[23, 24]. Understanding the internalization mechanisms can help us design a LDH-DNA bioconjugates with high penetration capacity and can explain the fundamental mechanism of these gene carriers. However, classic cytological approaches cannot report the exact mechanisms of the PM-LDH interaction and the internalization process of LDH nanosheets in a PM.

Recently, dissipative particle dynamics (DPD) simulations have been a good method to bridge the gap between the microscopic and the macroscopic scale. It can complement the lack of the nanoscale dynamic information within the experiment. It can be regarded as a coarse-grained molecular dynamics method that is suitable for large time and length scales. The DPD simulation is one of the most commonly used computer simulation techniques for the study of biomembrane systems[25-27] including the interactions between the biomembranes and nanoparticles[28, 29]. Mesoscopic simulation methods have been successfully applied to study the internalization mechanism of different nanoparticles[30-32].

Here, we investigated the internalization behavior of the LDH-DNA bioconjugates into plant cells by combining atomic force microscopy (AFM), confocal imaging, and

DPD simulations. We found that the DNA-LDH-DNA sandwich is the main form of all potential LDH-DNA bioconjugates after fully absorbing DNA molecules on delaminated LDH nanosheets. The DPD simulations revealed that the DNA-LDH-DNA sandwich enters the cell through a penetration pathway. Therefore, the DNA-LDH-DNA sandwich is an effective internalizable structure for LDH-DNA bioconjugates into plant cells. We believe that this work will provide new insights into the design of new gene delivery carriers.

2. Methods and experimental

2.1. Synthesis and Characterization

We used $\text{Mg}(\text{C}_3\text{H}_5\text{O}_3)_2 \cdot 3\text{H}_2\text{O}$, $\text{Al}(\text{C}_3\text{H}_5\text{O}_3)_3$ and $\text{C}_3\text{H}_6\text{O}_3$ to synthesize LDH-lactate. This was delaminated into single layers (LDH-lactate-NS) in decarbonated water. The entire process was carried out in a N_2 atmosphere at room temperature, and the pH was held at 10. After aging for 24 h under magnetic stirring, we centrifuged (5000 rpm, 8 min) the slurry and rinsed with decarbonated water until the sample became slightly cloudy. Finally, the sample was dried under vacuum at room temperature. Subsequently, the LDH-lactate was put into decarbonated water followed with stirring until it became transparent. More details can be found in our previous work[24].

The XRD patterns were recorded on a Shimadzu XRD-6000 instrument in reflection mode with Cu K radiation. The accelerating voltage was 40 kV with 30 mA current ($\lambda = 1.542\text{\AA}$) at 0.1° s^{-1} from 5° to 65° . Tapping mode AFM images were acquired under ambient conditions by directly casting sample dispersions onto freshly cleaved mica sheets using a Shimadzu SPM-9600 AFM system with Pico scan v 5.3.3 software. Confocal laser scanning microscopy (Leica SP8, Germany) was used to image the

intracellular fluorescence. The fluorescein isothiocyanate isomer I (FITC) labelled samples were excited with 488 nm laser and the emission fluorescence was collected at wavelengths between 500–550 nm.

2.2. Preparation of LDH-DNA bioconjugates

FITC-labeled ssDNA was purchased from TaKaRa Biotech. Co., Ltd (Dalian, P. R. China) and dispersed in ddH₂O (Mili-Q) as an aqueous solution. We then gently mixed ssDNA-FITC and LDH-lactate-NS at weight ratios of 1:3 followed by a 15 min incubation to couple LDH-lactate-NS with ssDNA-FITC. It should be noted that the freshly synthesized LDH-lactate-NS should be tightly sealed to prevent the reconstruction of the delaminated LDH NS into LDH bulk. With good sealing, the synthesized LDH-lactate-NS can be used within 30 days[23].

2.3. Cell culture, cellular uptake, and confocal imaging

BY-2 cells (*Nicotianatobacum* cv Bright Yellow 2) were cultured in a standard growth medium containing 0.43% [w/v] Murashige and Skoog salts, 1 mg/L thiamine, 0.2 mg/L 2,4-D, 100 mg/L Myo-inositol, 0.255 g/L KH₂PO₄, and 3% [w/v] sucrose (pH 5.0). The BY-2 cells were put in an orbital shaker at 130 rpm and 26 °C in dark. After 3–4 days of cultivation, the cells were filtered with a cell strainer to obtain a well-dispersed cell suspension. This cell suspension was then incubated with LDH-lactate-NS-ssDNA-FITC. Control cells were incubated with the same amount of ssDNA-FITC. After incubation, the BY-2 cells were rinsed three times and then resuspended in a standard growth medium. We subsequently imaged the BY-2 cells using an inverted confocal microscope (Leica SP8, Germany). The samples were excited with 488 nm lasers, and the fluorescence was collected between 500–550 nm.

2.4. Dissipative particle dynamic simulation methods

The internalization mechanism for LDH-DNA bioconjugates was investigated by N-varied DPD simulation. DPD is one of the most commonly used computer simulation techniques to study biomembrane systems[33-35]. The framework of the N-varied DPD method uses beads i and j that interact with each other via a pairwise additive force consisting of a conservative force F_{ij}^C , a dissipative force F_{ij}^D , and a random force F_{ij}^R . Thus, the total force exerted on bead i can be expressed as $F_i = \sum_{i \neq j} (F_{ij}^C + F_{ij}^D + F_{ij}^R)$ (More details can be found in the Supporting Information).

The N-varied DPD method is a variant of the DPD method, in which the targeted membrane tension can be maintained by monitoring the number of lipids per area (LNPA) in a boundary region[32, 36]. In this technique, the boundary region of the membrane is a reservoir of the lipids. The value of the LNPA in the boundary region (denoted as ρ_{LNPA}^{BR}) is kept constant by deletion or addition, where $\rho_{LNPA}^{BR}=1.47$ corresponds to zero surface tension [26]. Unless specified, the surface tension of the membrane was set to zero surface tension $\rho_{LNPA}^{BR}=1.47$. The lipid molecule is constructed from a headgroup with three hydrophilic beads connected to two hydrophobic tails. Each has five hydrophobic beads as before[37]. There are usually many negatively charged lipids on the membrane. Herein, receptors were used to represent the negatively charged lipids. The molecular structure of the receptor is similar to that of the lipid. To simulate the electrostatic interaction between the receptor and LDH, there must be an attractive interaction between the LDH and the receptor.

2.5. Models

LDH is composed of hydrophilic beads that are constrained together to move as a rigid hexagonal structure. The ssDNA is a simple coarse grain in a helical structure. Three possible structures were designed to investigate the effective internalization complex structure of LDH and ssDNA. The first is that LDH was intercalated into two ssDNAs, which we simply called the DNA-LDH-DNA sandwich. The second is that ssDNA was adhered to the surface of the LDH, which we named as the DNA-LDH complex. The third is that the ssDNA was intercalated into two LDHs the LDH-DNA-LDH sandwich (Detail models are in the Supporting Information).

3. Results and Discussion

3.1 Effective delivery of DNA into the nucleus of BY-2 cells using LDH

Lactate intercalated layered double hydroxide (LDH-lactate) was used because it has high DNA absorption capacity and facile water delamination[21]. The single layered nanosheets (LDH-lactate-NS) were produced by delaminating synthesized LDH-lactate bulk in decarbonated water (Fig. 1a). Subsequently, AFM was used to visualize the morphology and thickness of the LDH-lactate and LDH-lactate-NS. Tapping-mode AFM images of LDH samples deposited on a mica substrate are shown in Figs 1b and c. Non-delaminated LDH-lactate has typical lamellar crystallite morphology with an average thickness of around 4 nm (Fig. 1b). After delamination, the LDH-lactate-NS was well-dispersed, and the thickness of those nanosheets ranged from 0.5 to 7 nm (Fig. 1c). The particle thickness reflects the degree of dispersion. The theoretical thickness of a single LDH nanosheet is 0.6–0.8 nm, and thick particles indicated an incomplete delamination of the LDH-lactate or restacking of delaminated LDH-lactate nanosheets

during sampling for imaging. AFM was also used to show the structure of LDH nanosheets after absorbing FITC-labeled single strand DNA (ssDNA-FITC) molecules, the so-called LDH-DNA bioconjugates. AFM images of ssDNA-FITC, LDH-lactate-NS and LDH-DNA bioconjugates are shown in Figs 2a-c, respectively. The results indicated that the ssDNA-FITC have different height values that range from 1.2 to 5 nm. And the measured thickness on the filament region is 2.8 nm (Fig. 2a). Given that the theoretical height of ssDNA is about 2 nm[38], the measured height may reflect the stretching, twisting, and restacking of ssDNA-FITC. After incubation of ssDNA-FITC with LDH-lactate-NS at a concentration that enables LDH-lactate-NS saturation with DNA molecules[21], we found that the thickness of LDH ranges from 5 to 15 nm (Fig. 2c). To verify the different structures of these LDH-DNA bioconjugates, the surface profiles of the LDH-lactate-NS and these bioconjugates were measured. Figure 2d shows that a typical LDH-lactate-NS has a thickness of 0.8 nm and flat surface. For the LDH-lactate-NS absorbed DNA molecules, three different populations were found. The particles have about 4 nm thickness could reflect a DNA-LDH complex, which showed a fluctuated surface (blue line in Fig 2e). The 5 nm thick particles may reflect the LDH-DNA-LDH sandwich complex with a flat surface (green line in Fig 2e). The 8 nm thick particles may reflect the DNA-LDH-DNA complex, and the curve is fluctuated again (red line in Fig 2e). The measured particles from AFM images were shown in Supplemental Fig. 1. All these schematic structures are shown in Fig. 2f.

X-ray diffraction analysis was further used to define the formation of LDH-DNA bioconjugates because the sedimentation of LDH-DNA bioconjugates for AFM studies may cause restacking. The XRD patterns of dried LDH-lactate (Fig. 2g black curve)

shows the typical LDHs phases with $00l$ Bragg reflections at low 2θ values and broad and asymmetrical reflections at higher angles. After delamination, the characteristic diffractions of LDH-lactate structure disappeared. There were no sharp basal plane reflections, which suggest that the host sheets are not coherently stacked together to induce X-rays diffraction. This indicates that the LDH-lactate was delaminated into individual nanosheets (Fig. 2g blue curve)[39]. In the sample of LDH-DNA bioconjugates, the XRD pattern showed no $00l$ Bragg reflections. This confirmed that the LDH-DNA bioconjugates were still in a well-exfoliated state after adsorbing DNA (Fig. 2g red curve). These results indicated that the well-dispersed DNA-LDH-DNA sandwich complex with a single layer is the main product in the suspension. However, small amounts of other potential LDH-DNA bioconjugates including the DNA-LDH complex and the LDH-DNA-LDH sandwich complex cannot be excluded.

3.2. The internalization mechanism and effective internalization structure for the LDH-DNA bioconjugates by DPD simulations.

The LDH-lactate-NS can transport membrane impermeable fluorescent dyes and ssDNA molecules into the cytosol of both animal and plant cells[21, 22, 24]. Here, we also present experimental evidence that the LDH-lactate-NS can freely penetrate the cell wall of intact plant cells and transport the ssDNA-FITC molecules within nucleus, while the ssDNA-FITC itself is membrane impenetratable (Fig. 3). Without the process of delamination, LDH-lactate cannot act as molecular carrier in intact plant cells (data not shown), suggesting that the cell wall may act as a physical barrier to high level LDH aggregates. To investigate the internalization mechanism and effective internalization structure for LDH-DNA bioconjugates, the kinetics of the internalization process for

three simple bioconjugate structures were studied by DPD simulations. To distinguish these, we named these three possible LDH-DNA bioconjugate structures as DNA-LDH-DNA sandwich complex, DNA-LDH complex, and LDH-DNA-LDH sandwich complex. The generic terms of the three possible bioconjugates structure are LDH-DNA bioconjugates.

The internalization kinetics of the DNA-LDH-DNA sandwich complex were first investigated with three different initial orientations including $\varphi_0 = 0^\circ, 45^\circ, 90^\circ$, respectively. The DNA-LDH-DNA was initially placed in the position close to the lipid membrane. When the initial orientation of the DNA-LDH-DNA was vertical to the normal of the membrane ($\varphi_0 = 90^\circ$), the DNA-LDH-DNA gradually rotates itself and partly penetrates into the lipid membrane (1600 ns) (Fig. 4a). At 6240 ns, the DNA-LDH-DNA was nearly completely covered with lipid molecules except for the top of the ssDNA. Finally, the top of the ssDNA hydrophobic sequences insert further into the lipid membrane to finish the penetration process (Fig. 4a, 9600 ns). Furthermore, different initial orientations of DNA-LDH-DNA showed similar penetration processes (Figs 4b and 4c) and a similar orientation change trend during penetration (Fig. 4d). This suggests that the initial orientation of the DNA-LDH-DNA did not affect their internalization pathways.

The kinetics of the DNA-LDH internalization was also studied using DPD simulations. A typical internalization process for DNA-LDH complex with an initial orientation angle of $\varphi_0 = 90^\circ$ is shown in Fig. 5a. The DNA-LDH complex rotated and inserted into the hydrophobic layers (Fig. 5a, 3200 ns). However, after the partial hydrophobic insertion, the DNA-LDH complex only adhered to the surface of the lipid

membrane (Fig. 5a, 6400 ns), but did not completely penetrate into the lipid membrane (Fig. 5a, 9600 ns). Furthermore, different initial orientations of the DNA-LDH complex ($\varphi_0 = 0^\circ, 45^\circ, 90^\circ$) did not affect the penetration process (Supplementary Fig. 2). In conclusion, the DNA-LDH complex is not an effective penetration structure for the LDH-DNA bioconjugates.

The internalization kinetics for LDH-DNA-LDH with different orientations was also investigated. When the initial angle is vertical to the normal of the membrane ($\varphi_0 = 90^\circ$) (Fig. 5b) due to the attractive interactions between LDH and the membrane, the LDH-DNA-LDH gradually rotated itself and adhered to the surface of the lipid membrane (Fig. 5b, 3200 ns). Later, the LDH-DNA-LDH was partially wrapped in a lipid membrane. Concurrently, some lipid molecules were inserted into the intermediate sandwich of LDH-DNA-LDH due to hydrophobic effects (Fig. 5b, 6400 ns). Finally, the LDH-DNA-LDH was partially wrapped in a lipid membrane, but it failed to fully endocytose after a long simulation time (Fig. 5b, 9600 ns). Different initial orientations of this complex ($\varphi_0 = 0^\circ, 45^\circ, 90^\circ$) did not affect the penetration processes (Supplementary Fig. 3). In conclusion, LDH-DNA-LDH is not an effective penetration structure for LDH-DNA bioconjugates.

3.3. The influence of the LDH-DNA bioconjugate's structure on membrane penetration.

The membrane penetration of the LDH-DNA bioconjugate can be explained nicely by analyzing the structures of the DNA-LDH-DNA sandwich complex, DNA-LDH complex and LDH-DNA-LDH sandwich complex especially their physical features. Usually, due to the electrostatic repulsion between the negatively charged lipid membrane

and the negatively charged DNA, bare DNA is difficult to deliver to the cell. However, LDH nanosheets have positively charged surface and can neutralize the negatively charged DNA. Therefore, the electrostatic repulsion between the negatively charged lipid membrane and the DNA was weakened[24]. On the other hand, when the negatively charged DNA sequences were interacted and wrapped with the positively charged LDH, a flexible DNA chain could leave the hydrophobic sequences of the DNA exposure on the outside. The hydrophobic sequences of DNA can provide a driving force for penetration. For example, the DNA-LDH-DNA sandwich complex will be gradually inserted into the membrane to minimize exposure of the DNA hydrophobic sequences in the hydrophilic solvent.

In our experimental studies, we found that the LDH bioconjugates internalization was not reduced by endocytosis inhibitors or low temperatures[24]. This suggests that LDH-lactate-NS penetrated the plasma membrane via non-endocytic pathways. In our experiment, DNA is excessive versus the LDH-lactate-NS during adsorption. Furthermore, the AFM and XRD results indicated that the DNA-LDH-DNA sandwich complex is the most abundant form in suspension. We confidently conclude that the free penetration of the DNA-LDH-DNA sandwich complex is a mainstream for LDH-based DNA delivery into cells. This agrees with our early experimental data. This result suggests that excessive DNA concentrations during LDH adsorption benefits the formation of a DNA-LDH-DNA sandwich complex and can effectively improve the penetration capability of LDH-DNA bioconjugates.

On the other hand, the DNA-LDH complex first rotates to the hydrophobic insert. However, after a partial hydrophobic insert, the DNA-LDH complex can only adhere to

the surface of the lipid membrane with LDH nanosheets. There is no further driving force for penetration, and the DNA-LDH complex can only partially penetrate and adhere to the lipid membrane rather than complete penetration. Besides, for the LDH-DNA-LDH sandwich complex, due to the attractive interaction between LDH nanosheets and lipid membrane. Thus lipid membrane can partially wrap the LDH-DNA-LDH sandwich complex. However, full wrapping and endocytosis of the LDH-DNA-LDH sandwich complex need to overcome large membrane bending energy. The LDH-DNA-LDH sandwich complex fails to be fully wrapped on this structure.

The simulation system is simpler than the in vivo system. Living cells have adaptor proteins and clathrin to form endosomes. And the plant cells have thick cell walls, which may avoid the high level aggregates from reaching the PM. In this condition, we also found that small amounts of LDH-FITC were colocalized within the clathrin-coated vesicles in living cells[24]. Therefore, the endocytotic pathways could play less important roles in the transmembrane transport of the LDH-DNA-LDH sandwich complex. Usually, the LDH-DNA complex and LDH-DNA-LDH sandwich complex is more likely to form when the sufficient LDH is provided during adsorption. This further suggests that abundant DNA is needed to form the membrane permeable DNA-LDH-DNA sandwiches in biochemical applications.

The internalization pathways of nanocarriers can determine the fate of the target molecules. The endocytosis pathway might lead to the combination within lysosomes or cystic vacuoles, in which the biomolecules are destroyed and degraded. On the other hand, internalization via free penetration can directly release the target molecules into the cytosol. Importantly, the DNA released into the cytosol can get into the nucleus through

the nuclear pore complex[40]. We also found that the LDH delivery of fluorescent markers within the cytosol via non-endocytic pathways and a prolonged incubation causes a significant accumulation of ssDNA-FITC within the nucleus[24].

4. Conclusion

In summary, we observed the formation of LDH-DNA bioconjugates by AFM and XRD analyses, which indicated that the DNA-LDH-DNA sandwich complex is the most abundant type of bioconjugate in these suspensions. The DPD simulations show that the DNA-LDH-DNA sandwich complex can freely penetrate the plasma membrane with high efficiency. This agrees well with our early experimental studies, which suggest that the LDH can transport target into cytosol via a non-endocytic pathway. The free penetration of nanocarriers offered several advantages including high efficiency, low specificity, and preventing the target molecules from lysosome degradation, which therefore enable the LDH deliver the ssDNA-FITC into the nucleus. The membrane penetration capacity of DNA-LDH complex and LDH-DNA-LDH sandwich complex were also evaluated and none of them could penetrate the membrane via free penetration, but the LDH-DNA-LDH initiates tend to endocytosis. The simulation system cannot include all *in vivo* factors, and thus we cannot simply exclude the role of endocytotic pathways in the uptake of LDH-DNA-LDH. Taken together, we combined experimental and computational approaches to discover the molecular mechanism of LDH-DNA bioconjugates to cells. We are confident that our work can provide a new guidance for the design of highly effective LDH-based DNA delivery.

Acknowledgements

This work is supported by the Fundamental Research Funds for the Central Universities(2016JX01, BLX2015-01), the National Natural Science Foundation of China (31671489, 31601149 and 31271433), the Beijing Nova Programme (Z131109000413013). Special Program for Applied Research on Super Computation of the NSFC-Guangdong Joint Fund (the second phase) and Chemical Grid Program and Excellent Talent of BUCT.

References

- [1] Yang Y, Liu J, Sun X, et al. Near-infrared light-activated cancer cell targeting and drug delivery with aptamer-modified nanostructures. *Nano Res* 2016; 9:139-48.
- [2] Muroski ME, Carnevale KJ, Riskowski RA, et al. Plasmid transfection in mammalian cells spatiotemporally tracked by a gold nanoparticle. *ACS nano* 2015; 9:124-33.
- [3] Doorley GW, Payne CK. Cellular binding of nanoparticles in the presence of serum proteins. *Chem Commun* 2011; 47:466-8.
- [4] Kim ST, Saha K, Kim C, et al. The role of surface functionality in determining nanoparticle cytotoxicity. *Acc Chem. Res.* 2013; 46:681-91.
- [5] Shi X, von Dem Bussche A, Hurt RH, et al. Cell entry of one-dimensional nanomaterials occurs by tip recognition and rotation. *Nat Nanotechnol* 2011; 6:714-19.
- [6] Liu Q, Chen B, Wang Q, et al. Carbon nanotubes as molecular transporters for walled plant cells. *Nano Lett* 2009; 9:1007-10.
- [7] Serag MF, Kaji N, Gaillard C, et al. Trafficking and subcellular localization of multiwalled carbon nanotubes in plant cells. *ACS nano* 2010; 5:493-99.
- [8] Choi CHJ, Hao L, Narayan SP, et al. Mechanism for the endocytosis of spherical nucleic acid nanoparticle conjugates. *Proc Natl Acad Sci* 2013; 110:7625-30.
- [9] Liang J, Chen P, Dong B, et al. Ligand–Receptor Interaction-Mediated Transmembrane Transport of Dendrimer-like Soft Nanoparticles: Mechanisms and Complicated Diffusive Dynamics. *Biomacromolecules* 2016; 17:1834-44.
- [10] El-Sayed A, Harashima H. Endocytosis of gene delivery vectors: from clathrin-dependent to lipid raft-mediated endocytosis. *Molecular Therapy* 2013; 21:1118-30.
- [11] Mäe M, Myrberg H, Jiang Y, et al. Internalisation of cell-penetrating peptides into tobacco protoplasts. *Biochimica et Biophysica Acta (BBA)-Biomembranes* 2005; 1669:101-07.
- [12] Rosenbluh J, Singh SK, Gafni Y, et al. Non-endocytic penetration of core histones into petunia protoplasts and cultured cells: a novel mechanism for the introduction of

macromolecules into plant cells. *Biochimica et Biophysica Acta (BBA)-Biomembranes* 2004; 1664:230-40.

[13]Lim Y-b, Kim S-m, Suh H, et al. Biodegradable, endosome disruptive, and cationic network-type polymer as a highly efficient and nontoxic gene delivery carrier. *Bioconjugate Chemistry* 2002; 13:952-57.

[14]Pattni BS, Chupin VV, Torchilin VP. New developments in liposomal drug delivery. *ChemRev* 2015; 115:10938-66.

[15]Hu Y, Litwin T, Nagaraja AR, et al. Cytosolic delivery of membrane-impermeable molecules in dendritic cells using pH-responsive core-shell nanoparticles. *Nano Lett* 2007; 7:3056-64.

[16]Chen M, Cooper HM, Zhou JZ, et al. Reduction in the size of layered double hydroxide nanoparticles enhances the efficiency of siRNA delivery. *J Colloid Interface Sci* 2013; 390:275-81.

[17]Ladewig K, Niebert M, Xu ZP, et al. Efficient siRNA delivery to mammalian cells using layered double hydroxide nanoparticles. *Biomaterials* 2010; 31:1821-29.

[18]Gu Z, Rolfe BE, Thomas AC, et al. Cellular trafficking of low molecular weight heparin incorporated in layered double hydroxide nanoparticles in rat vascular smooth muscle cells. *Biomaterials* 2011; 32:7234-40.

[19]Oh J-M, Kwak S-Y, Choy J-H. Intracrystalline structure of DNA molecules stabilized in the layered double hydroxide. *J Phys Chemif Solids* 2006; 67:1028-31.

[20]Wong Y, Markham K, Xu ZP, et al. Efficient delivery of siRNA to cortical neurons using layered double hydroxide nanoparticles. *Biomaterials* 2010; 31:8770-79.

[21]Wang J, Bao W, Umar A, et al. Delaminated Layered Double Hydroxide Nanosheets as an Efficient Vector for DNA Delivery. *J Biomedical Nanotech* 2016; 12:922-33.

[22]Li S, Li J, Wang CJ, et al. Cellular uptake and gene delivery using layered double hydroxide nanoparticles. *J MaterChem B* 2013; 1:61-68.

[23]Mitter N, Worrall EA, Robinson KE, et al. Clay nanosheets for topical delivery of rna for sustained protection against plant viruses. *Nat Plants* 2017; 3.

[24]Bao W, Wang J, Wang Q, et al. layered double hydroxide nanotransporter for molecule delivery to intact plant cell. *Sci Rep* 2016; 6.

[25]Shillcock JC, Lipowsky R. Tension-induced fusion of bilayer membranes and vesicles. *Nature Mater* 2005; 4:225-28.

[26]Yue T, Li S, Zhang X, et al. The relationship between membrane curvature generation and clustering of anchored proteins: a computer simulation study. *Soft Matter* 2010; 6:6109-18.

[27]Chen X, Tian F, Zhang X, et al. Internalization pathways of nanoparticles and their interaction with a vesicle. *Soft Matter* 2013.

[28]Li Y, Zhang X, Cao D. A spontaneous penetration mechanism of patterned nanoparticles across a biomembrane. *Soft Matter* 2014; 10:6844-56.

[29]Li Y, Zhang X, Cao D. Nanoparticle hardness controls the internalization pathway for drug delivery. *Nanoscale* 2015; 7:2758-69.

- [30]Ma Y-q. pH-responsive dendrimers interacting with lipid membranes. *Soft Matter* 2012; 8:2627-32.
- [31]Yang K, Ma Y. Computer simulation of the translocation of nanoparticles with different shapes across a lipid bilayer. *Nature Nanotech* 2010; 5:579-83.
- [32]Li Y, Yue T, Yang K, et al. Molecular modeling of the relationship between nanoparticle shape anisotropy and endocytosis kinetics. *Biomaterials* 2012; 33:4965-73.
- [33]Yang K, Yuan B, Ma Y-q. Influence of geometric nanoparticle's rotation on cellular internalization Process. *Nanoscale* 2013;5:7998-8006.
- [34]Alexeev A, Uspal WE, Balazs AC. Harnessing Janus nanoparticles to create controllable pores in membranes. *ACS nano* 2008; 2:1117-22.
- [35]Yang K, Ma Y-Q. Computer simulation of the translocation of nanoparticles with different shapes across a lipid bilayer. *Nature Nanotech* 2010; 5:579-83.
- [36]Yue T, Zhang X. Cooperative effect in receptor-mediated endocytosis of multiple nanoparticles. *ACS nano* 2012; 6:3196-205.
- [37]De Meyer FJM, Venturoli M, Smit B. Molecular simulations of lipid-mediated protein-protein interactions. *Biophys J* 2008; 95:1851-65.
- [38]watson JD, crick F.H.C. molecular structure in nucleic acids: a structure for deoxyribose nucleic acids. *Nature* 1953; 171:737-38.
- [39]Wang J, Huang L, Gao Y, et al. A simple and reliable method for determining the delamination degree of nitrate and glycine intercalated LDHs in formamide. *Chem Commun (Camb)* 2014; 50:10130-2.
- [40]Greber UF, Suomalainen M, Stidwill RP, et al. The role of the nuclear pore complex in adenovirus DNA entry. *The EMBO journal* 1997; 16:5998-6007.

Figures

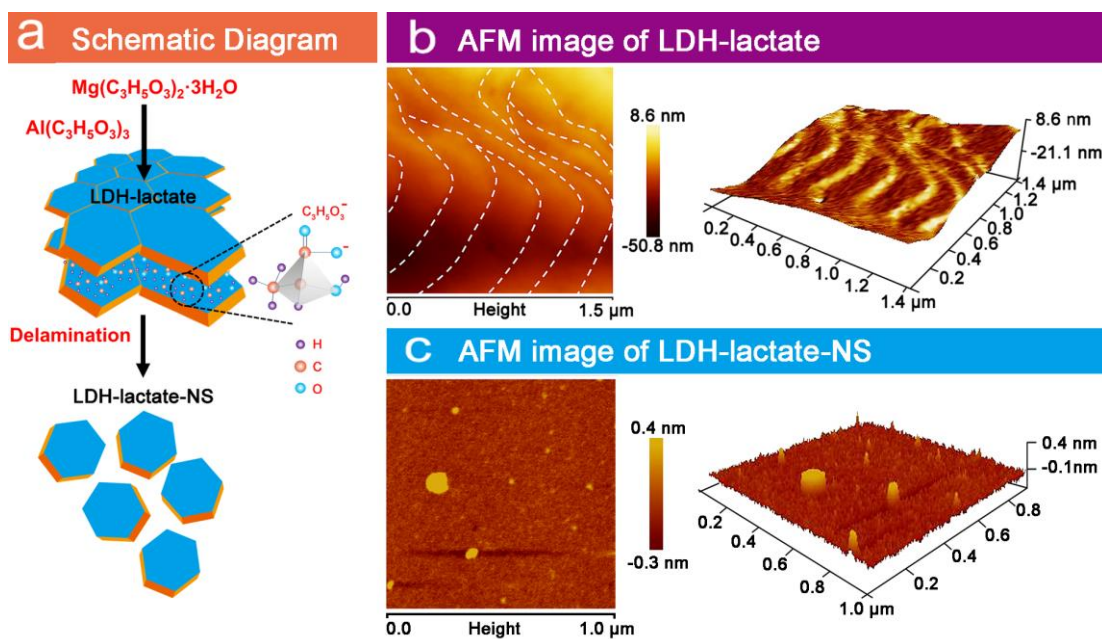


Figure 1. Schematic diagram and characterization. (a) Schematic diagram for the synthesis and delamination of LDH-lactate, (b) AFM image of LDH-lactate, and (c) AFM image of LDH-lactate-NS.

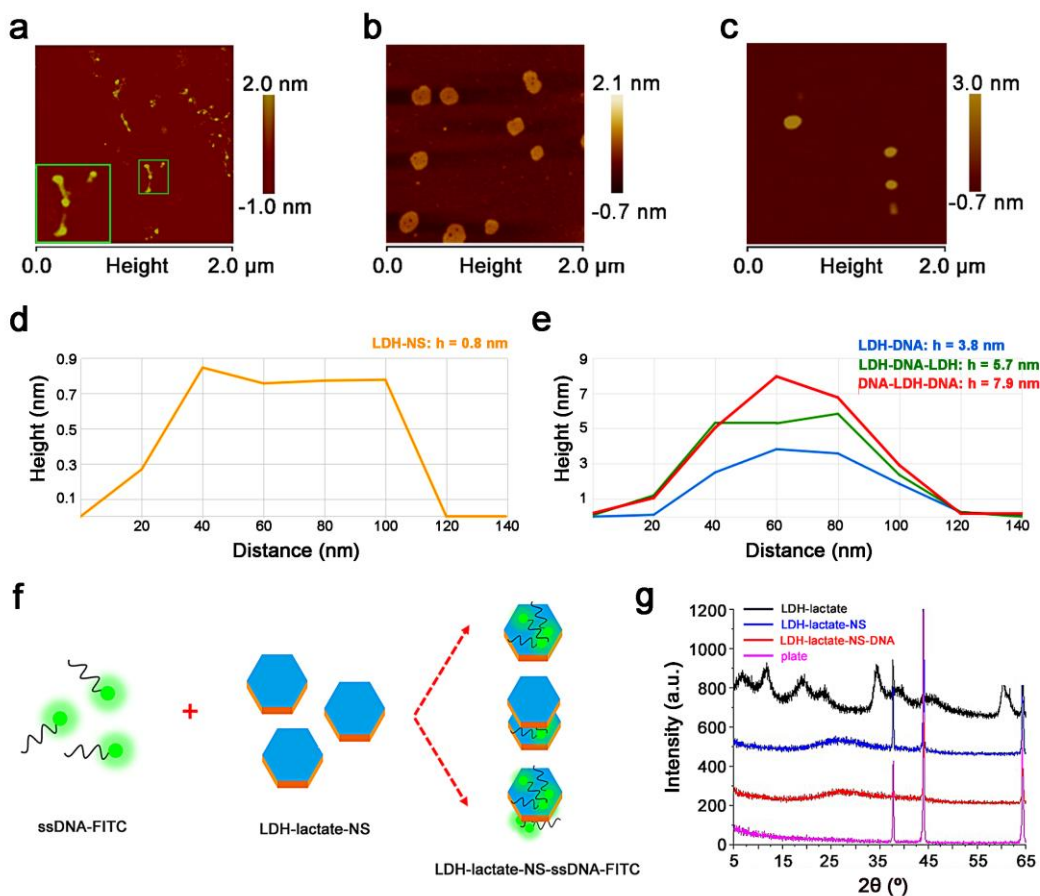


Figure 2. Characterization of nanosheets and biomolecular structure. AFM image of (a) ssDNA-FITC and zooming one of tadpole-like ssDNA-FITC in corresponding box circled with green frame, the measured thickness of ssDNA is 2.8 nm, (b) LDH-lactate-NS, and (c) LDH-DNA bioconjugates, (d) section profile of a LDH-lactate-NS, the measured thickness is 0.8 nm, (e) section profiles of LDH-DNA bioconjugates, showing three typical alteration of thickness, h: height, d: diameter, (f) schematic diagram of the conjugation pathway of ssDNA-FITC, LDH-lactate-NS and postulated structures of LDH-DNA bioconjugates, (g) XRD patterns of LDH-lactate, LDH-lactate-NS, LDH-lactate-NS-DNA, and an empty sample plate.

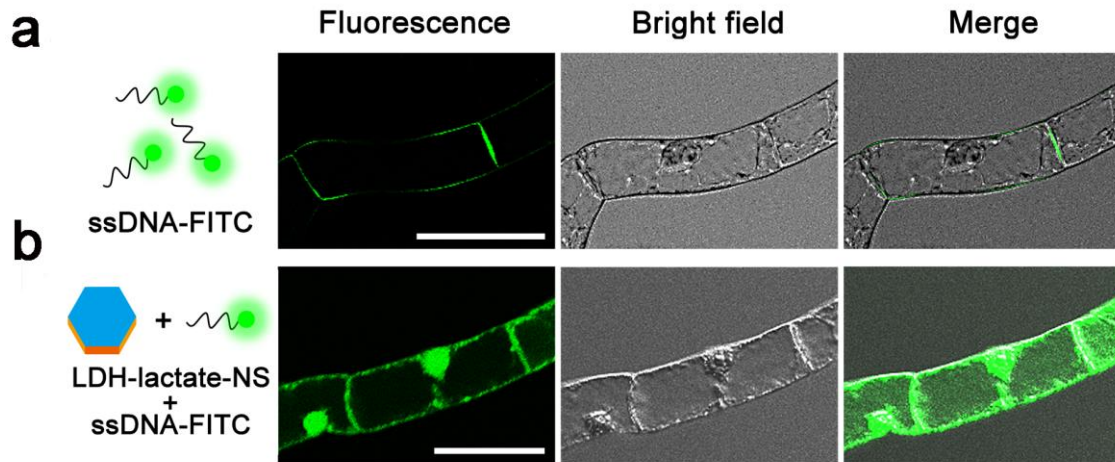


Figure 3. Penetration of LDH-DNA bioconjugates into BY-2 suspension cells. (a) BY-2 cells were incubated in the ssDNA-FITC containing medium for 60 minutes, (b) BY-2 cells were incubated within medium containing ssDNA-FITC conjugated LDH-lactate-NS for 60 minutes. Scale bars = 50 μ m.

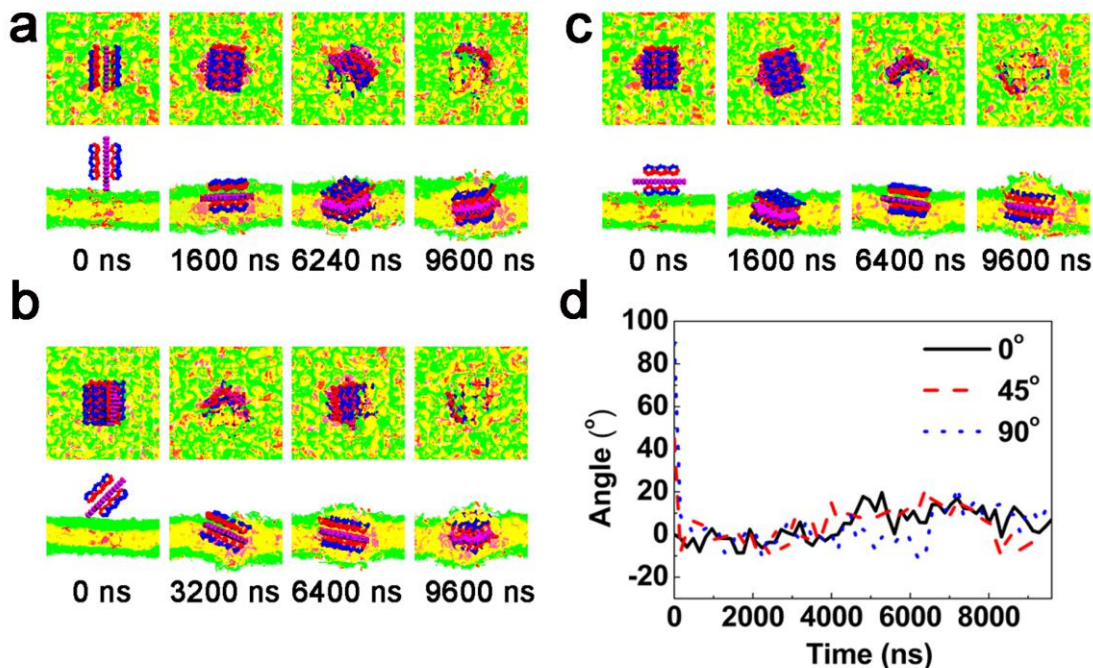


Figure 4. Several typical snapshots of the penetration simulation processes of DNA-LDH-DNA complex in different initial orientations. In the snapshots, the lipid head is shown in green, the lipid tail in yellow, the receptor head in pink, the receptor tail in orange, the hydrophobic component of DNA is shown in blue, the hydrophilic component of DNA is shown in red, and LDH is shown in purple; water molecules are not shown in the snapshots for clarity. The initial orientations of DNA-LDH-DNA sandwich complex are (a) 90°, (b) 45°, and (c) 0°, (d) time evolution for the complexes of DNA-LDH-DNA orientation.

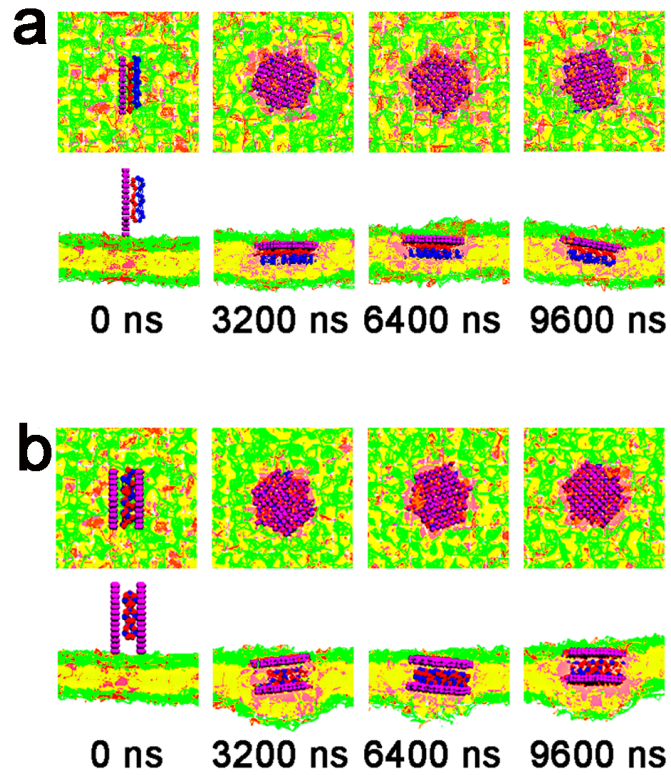


Figure 5. Several typical snapshots for the penetration simulation processes. (a) DNA-LDH complex and (b) LDH-DNA-LDH sandwich complex with an initial orientation 90° . In the snapshots, the color code is the same as in Fig. 4.